

Article

# Curcumin-Loaded Nanoemulsion for Better Cellular Permeation

Nur Hulwani Md Saari <sup>1,2</sup>, Lee Suan Chua <sup>1,2,\*</sup> , Rosnani Hasham <sup>1,2</sup>  and Leny Yulianti <sup>3</sup> 

<sup>1</sup> Institute of Bioproduct Development, Universiti Teknologi Malaysia, UTM Skudai, Johor Bahru, Johor 81310, Malaysia; wani24434@yahoo.com (N.H.M.S.); r-rosnani@utm.my (R.H.)

<sup>2</sup> Department of Bioprocess and Polymer Engineering, School of Chemical and Energy Engineering, Faculty of Engineering, Universiti Teknologi Malaysia, UTM Skudai, Johor Bahru, Johor 81310, Malaysia

<sup>3</sup> Ma Chung Research Center for Photosynthetic Pigments, Universitas Ma Chung, Malang 65151, Indonesia; leny.yulianti@machung.ac.id

\* Correspondence: chualesuan@utm.my; Tel.: +60-19-721-4378

Received: 30 August 2020; Accepted: 28 September 2020; Published: 6 October 2020



**Abstract:** Curcumin nanoemulsion was prepared using coconut oil, Tween 80 (surfactant) and polyethylene glycol (co-solvent) with the addition of honey and glycerol as additives. The nanoemulsion was optimized and systematically characterized for transdermal delivery. Small particle size (15.92 nm), low polydispersity index (0.17) and slight acidic (pH 4.18) curcumin nanoemulsion was obtained without any chemical degradation based on the Fourier transform infrared (FTIR) spectrum. The incorporation of curcumin inside nanoglobul improved curcumin stability and skin permeability. Its high permeability can be seen from Nile dyed curcumin in different layers of skin through fluorescent imaging. The release kinetic of curcumin followed the Higuchi model, which explains why the skin permeation was a Fickian diffusion-controlled process because the Korsmeyer constant was proven to be 0.3 (<0.5). Nanoencapsulation slightly decreased the antioxidant capacity of curcumin for about 7.9% compared to its free counterpart. It showed low cytotoxicity (EC<sub>50</sub> 2.3552 µg/mL) to human skin fibroblasts. Cell death was noticed at a high concentration (2.5 µg/mL) of treatment. Curcumin was also found to promote wound closure at low concentration 0.1563 µg/mL and was comparable with the performance of ascorbic acid based on scratch assay. Therefore, this nutritious curcumin nanoemulsion is a promising transdermal delivery system for topical application.

**Keywords:** nanoparticles; natural product; kinetic; controlled release; permeability

## 1. Introduction

Curcumin is a lipophilic bioactive compound that can be found in the rhizome of *Curcuma longa* Lin from the ginger family, Zingiberaceae. It is commonly used as folk medicine and considered to be safe as nutritional dietary food. Previous studies reported that curcumin appeared to be a hepatoprotective and nephroprotective agent [1]. Therefore, the compound has been received immense attention over the past decades, mainly because of its diverse biological activities, including anticancer, antioxidant, anti-amyloid, anti-inflammatory, antidiabetic, antibiotic, and antiviral activities [2]. Although curcumin is a potent radical scavenger, it possesses low bioavailability, instability during processing and poor solubility in aqueous solution. The drawbacks may lead to poor absorption of the active compound in human body.

Several attempts have been carried out to encapsulate curcumin with a protective layer for better functionality in cosmeceutical, pharmaceutical and functional food industries. This includes the use of different vegetable oils, surfactants/co-surfactants and co-solvents to increase the stability and permeability of curcumin. Studies found that the delivery system of nanoemulsion loaded with 1% curcumin was sufficient to treat acute and chronic toxoplasmosis in mouse models [3]. High stability of nanoencapsulated curcumin could also be seen from the stimulated gastrointestinal studies. Curcumin encapsulated by medium-chain triglyceride oil was resistant to pepsin digestion [4]. Curcumin nanoemulsion could also enhance transdermal delivery by increasing permeation flux and release kinetics to accelerate wound healing. Previous studies proved that the release kinetics of curcumin was controlled by the diffusion following Higuchi model [5,6]. In vitro assays revealed that curcumin nanoemulsion was safe for normal human cells, but favorably cytotoxic to cancerous gastric, colon, breast and melanoma cells [7,8]. This indicates high selectivity of curcumin nanoemulsion against cancer cells, but low cytotoxicity to normal cells.

The present study optimized the formulation of curcumin encapsulation in the form of nanoemulsion. Natural, nutritious and nontoxic ingredients would be of primary choice. Therefore, honey and coconut oil were selected for the aqueous and oil phases, respectively, for curcumin-loaded nanoemulsion. Tween 80 was used as non-ionic surfactant in the emulsification of oil-in-water since it was reported to have no adverse effects. The quality of encapsulated nano-sized curcumin was systematically evaluated based on the physiochemical characteristics, antioxidant capacity, cytotoxicity, release kinetic of skin permeation, and wound healing property compared to its free counterpart.

## 2. Materials and Methods

### 2.1. Chemicals

Natural Tualang honey, which was in dark yellow with a pH of 3.8 and a moisture content of 23.3%, was purchased from the Federal Agricultural Marketing Authority (FAMA, Kuala Nerang, Kedah, Malaysia). Virgin coconut oil (VCO) was obtained from the Institute of Bioproduct Development, Universiti Teknologi Malaysia (Skudai, Malaysia) with the moisture content less than 0.5%. Curcumin ( $\geq 98.0\%$ ), glycerol ( $\geq 99\%$ ), phosphate-buffered saline (pH 6.5), Folin–Ciocalteu’s phenol reagent (2 N), DPPH (2,2 diphenyl-1-picrylhydrazyl) and allantoin were sourced from Sigma-Aldrich (St. Louis, MO, USA). Tween 80, polyethelene glycol (PEG) 400, dimethyl sulfoxide (DMSO), methanol and ethanol were purchased from Merck (Darmstadt, Germany). 3-(4,5-dimethylthiazole-2-yl)-2,5-diphenyl tetrazolium (MTT), fetal bovine serum (FBS), Dulbecco’s Modified Eagle’s Medium (DMEM) and 1% penicillin with streptomycin, trypsin-EDTA were bought from Life Technology Corporation (Carlsbad, USA). Sprague Dawley rats between 200 and 250 g body weight at the age 8–9 weeks were purchased from Takrif Bestari Enterprise (Selangor, Malaysia). Human skin fibroblast cells (HSF 1184) were purchased from Life Technology Bio Diagnostic (Kuala Lumpur, Malaysia).

### 2.2. Preparation of Curcumin-Loaded Nanoemulsion

Nanoemulsion was prepared by using a spontaneous emulsification technique. Different percentages of VCO (1–13% *w/w*) and its surfactant, Tween 80 (5–9%), were mixed and stirred at 400 rpm and 25 °C for 30 min. Honey (0.5–5.0 g) which was premixed with 3% glycerol was slowly added into the oil phase solution with continuous stirring. Distilled water was then added to mark up the total volume of nanoemulsion to 100 mL. After being stored for 24 h at 25 °C, the prepared nanoemulsion was visualized and analysed for its turbidity using a spectrophotometer (UV-1800, Shimadzu Corporation, Japan) at 425 nm. Only nanoemulsion with no phase separation and optically transparent was loaded with curcumin.

The composition of the nanoemulsion formulation was further optimized by introducing curcumin as a bioactive compound. Curcumin (10 mg) was premixed with PEG as co-surfactant and sonicated for 10 min at 45–50 °C. The curcumin solution was slowly added into the oil phase solution composed of VCO and Tween 80 and then stirred for 20 min. Honey which was added with 3% glycerol was then slowly added into the mixture and continuously stirred to obtain a clear and homogenous isotropic solution.

### 2.3. Morphological Characterisation

A Zetasizer Nano S (Malvern instrument, UK) was used to measure particle size, polydispersity index and zeta potential of nanoemulsion. The surface morphology of curcumin-loaded nanoemulsion was determined by transmission electron microscopy (TEM). The sample (10 mL) was dropped onto a 200-mesh grid and uranyl acetate (10 mL) was added on top of the grid. Excessive droplet was carefully removed using filter paper and left for drying. The sample was observed under a high-resolution transmission electron microscope (Hitachi HT7700, Tokyo, Japan).

### 2.4. Chemical Characterisation and Antioxidant Activity

Free curcumin and curcumin-loaded nanoemulsion were scanned in the wavenumber of 400–4000  $\text{cm}^{-1}$  using a Fourier transform infrared spectrometer (FTIR, PerkinElmer, Norwalk, CT, USA). Each spectrum was produced by 16 scans at a resolution of 4  $\text{cm}^{-1}$ .

The antioxidant activity of samples was determined using colorimetric DPPH assay. The antioxidative sample reduced purple coloured free radicals of DPPH into a more stable pale-yellow complex. The DPPH solution (0.01 mM) was dissolved in DMSO, and 0.5 mL of the solution was added into 1.5 mL of samples at different concentrations (0.15–0.45  $\mu\text{g}/\text{mL}$ ). The mixture was vortexed and incubated in a dark place for 30 min. After incubation, the absorbance of samples was recorded at 517 nm using a UV-Vis spectrophotometer (Shimadzu UV-1800, Kyoto, Japan). The result was expressed in  $\text{EC}_{50}$ , which is the amount of antioxidative sample required to inhibit 50% of radical DPPH.

The same concentration of curcumin either in the form of free curcumin or nanoencapsulated curcumin was prepared for the DPPH assay. Curcumin nanoemulsion was filtered through a mini spin column (Sephadex G-50) by centrifugation at 5 rpm for 5 min. The filtered solution (1 mL) was added into DMSO (1 mL) and homogenized before being filtered using a 0.45  $\mu\text{m}$  nylon syringe filter (13 mm). The concentration of encapsulated curcumin was determined using the calibration curve of standard curcumin. The calibration curve was constructed from the absorbance of standard curcumin at different concentrations ranged from 1–8  $\mu\text{g}/\text{mL}$ .

### 2.5. In Vitro Skin Permeation of Nano-Encapsulated Curcumin

A vertical Franz cell, which was purchased from PermeGear (OA60AP-22, Hellertown, USA) was fitted with the excised rat skin with an effective permeation area of 1.5  $\text{cm}^2$ . The skin was excised and then clamped between the donor and the receptor chambers. The skin was placed on the receiver chamber with the stratum corneum facing upward, and the donor chamber was next clamped in place. The receptor compartment was filled up with PBS buffer (pH 6.5) and the donor compartment was filled up with 1.25 mL curcumin-loaded nanoemulsion. The rat skin was mounted between the two compartments where the outer part of the skin was facing the donor compartment. The receptor chamber was thermostated at 37 °C using a re-circulating water bath. The fluid in the donor and receptor compartments were constantly stirred at 300 rpm for 30 min before the test sample (1.25 mL) was pipetted into the donor compartment and then sealed with paraffin. Aliquot (1 mL) was withdrawn from the receptor compartment at the pre-determined time intervals for 24 h. The same amount of fresh buffer (1 mL) was immediately replenished after the withdrawal. The release of curcumin into the receptor compartment was determined using a UV-Vis spectrophotometer at 420 nm. Ethanol (50% *v/v*) was added into the withdrawn sample to increase solubility of curcumin for measurement.

### 2.6. Fluorescent Imaging of Permeated Curcumin

Since curcumin has an innate fluorescent property, its localization at different depths of skin could be observed by fluorescent imaging. The skin sample was washed with PBS and dried gently with a towel. It was cut into approximately 1 cm<sup>2</sup> and placed in a clean beaker. Nile red was carefully added onto the skin sample that was placed on dry ice before keeping in a cryostat to freeze at –80 °C. The skin sample that was treated with PBS was used as a control experiment. The frozen skin sample was sectioned into 5 mm using a cryostat (Leica Inc., Wetzlar, Germany). One section from each group of samples was repeatedly treated with xylene to remove water and viewed under a fluorescent microscope (Olympus-BX-51, Tokyo, Japan).

### 2.7. Scratch Assay for Wound Healing

Fibroblast cells were seeded in 24-well plates at a density of  $3 \times 10^5$  cells/mL and then they were allowed to grow for 24 h at 37 °C and 5% CO<sub>2</sub>. A small linear scratch was created on the confluent monolayer of cells by gently scraping a straight line with a sterile pipette tip. Cells were then carefully rinsed with PBS to remove cellular debris before adding media with sample solution at different concentrations ranging from 0.1563 to 2.5000 µg/mL. Ascorbic acid (5 µg/mL) was used as a positive control and cells without treatment were used as a negative control. Images of migrated cells were taken using a digital camera connected to an inverted microscope (Axio Vert.A1, Zeiss, Germany) to observe the closure of wound area after 24 h.

### 2.8. Cell Cultivation and Proliferation Assay

Human skin fibroblasts were grown in DMEM supplemented with 10% heat inactive FBS, 1% penicillin and streptomycin. After reaching 90% confluency, the cells were washed with PBS buffer and seeded on a 96-well plate with a density of 10,000 cells per cm<sup>-2</sup>. The cells were maintained at 37 °C in a humidified atmosphere of 5% CO<sub>2</sub>. The cells were used to determine the cytotoxicity of samples using MTT assay. Different concentrations of curcumin-loaded nanoemulsion ranging from 0.16 to 2.50 µg/mL were used in the treatment for 24 h. The cell medium was removed using a pipette and the cells were carefully washed with PBS buffer. The viable cells were incubated with 20 µL MTT solution (5 mg/mL) for 4 h at 37 °C in a dark place. A 100 µL DMSO was added into each well to completely dissolve formazan crystals. Non-treated cells acted as negative control, and cells treated with ascorbic acid (5 µg/mL) and curcumin acted as positive control experiments. The optical density (OD) of sample solution was read in a microplate reader (Hidex, Turku, Finland) at 570 nm. The percentage of viable cells can be determined using Equation (1).

$$\text{Cell viability (\%)} = \frac{\text{OD (test)} - \text{OD (blank)}}{\text{OD (negative control)} - \text{OD (blank)}} \times 100 \quad (1)$$

## 3. Results

### 3.1. One-Factor-At-A-Time Optimization of Nanoemulsion Preparation

The preliminary data of nanoemulsion preparation were normalized and analyzed using a pseudoternary phase diagram in order to relate the phase interaction between oil phase, water phase and surfactant (Figure 1). The diagram shows to have a non-nano-sized emulsion region at a high ratio of VCO to Tween 80 and a low concentration of stabilizers (honey and glycerol). The increase in VCO would also increase the particle size of the nanoemulsion.

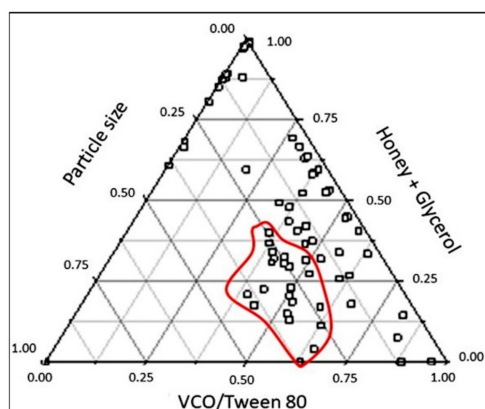


**Figure 1.** Ternary diagram of optimization for curcumin nanoemulsion formulation. The region of nano-sized particles is circled in red.

The one-time-at-a-time optimization process found that the formulation composed of 1% coconut oil, 9% Tween 80, 2% honey and 3% glycerol was selected as the base formulation for developing curcumin-loaded nanoemulsion. PEG (1%) was used as the co-solvent for better dissolution of curcumin (0.01%) in the nanoemulsion. The incorporation of curcumin had slightly shifted the optimized composition of nanoemulsion to be 1% coconut oil, 9% Tween 80, 2.4% honey and 3% glycerol. The curcumin-loaded nanoemulsion that was found to exhibit the particle size, 15.92 nm; low PDI, 0.171 and pH 4.18 was selected for the subsequent analysis. The spherical and globule nano-sized curcumin can also be seen evenly distributed in solution from the image of TEM (Figure 2). Visual inspection with no phase separation and microscopic evaluation based on the particle size were the main criteria of preparing this nutritious curcumin-loaded nanoemulsion.

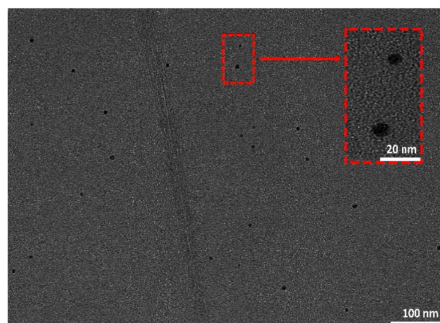


**Figure 2.** Curcumin-loaded nanoemulsion viewed under a transmission electron microscope with the magnification of 60,000 $\times$ .

### 3.2. FTIR Spectrum Analysis

The FTIR spectra of curcumin and curcumin-loaded nanoemulsion are presented in Figure 3. The spectrum of curcumin-loaded nanoemulsion was found to be similar to the pure curcumin, in which all the typical absorption peaks were present. The most important functional groups are O-H bending ( $1348.24\text{ cm}^{-1}$ ) and C=O stretching ( $1741.72\text{ cm}^{-1}$ ). The other bands in the region of  $2965\text{--}2855\text{ cm}^{-1}$  were contributed by the C-H stretching vibration, possibly due to the presence of O-C=O ( $2953.03\text{ cm}^{-1}$ ), O-H ( $2852.72\text{ cm}^{-1}$ ) and C-H ( $2922.16\text{ cm}^{-1}$ ) groups in curcumin-loaded nanoemulsion. The results are in agreement with the finding of Mohan et al. [9].

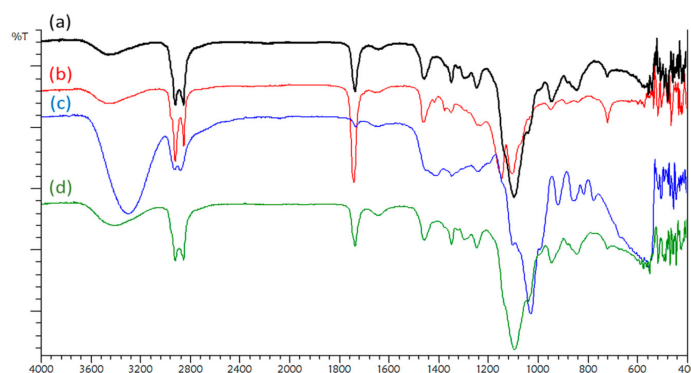


**Figure 3.** Fourier transform infrared (FTIR) spectra of (a) curcumin, (b) virgin coconut oil, (c) honey and (d) curcumin-loaded nanoemulsion.

The spectrum of virgin coconut oil shows the detection of dual peaks at  $2922.16$  and  $2854.65\text{ cm}^{-1}$  for asymmetric and symmetric C-H stretching, respectively (Figure 3b). The sharp dual peaks indicate that coconut oil consists mainly of linear carbon chain of fatty acids such as palmitic, lauric and stearic acids. Another sharp peak at  $1737.86\text{ cm}^{-1}$  represents carbonyl ester, whereas  $1247.86$  and  $1041.56\text{ cm}^{-1}$  are peaks assigned to the C-O stretching of fatty acids. There was no peak detected at  $3007$  and  $1655\text{ cm}^{-1}$  attributed to the stretching vibration of cis olefinic double bonds (C=C). Guillén and Cabo [10] explained that those peaks were indicators for unsaturated fatty acids such as oleic and linoleic acids in vegetable oils. The absence of those peaks explains that virgin coconut oil is composed of saturated fatty acid, especially lauric acid.

Tualang honey was found to have a strong and broad peak at  $3600\text{--}3000\text{ cm}^{-1}$  with the maximum value of  $3302.13\text{ cm}^{-1}$  (Figure 3c). The peak could be contributed by the O-H stretching of sugar polyols ( $3550\text{--}3200\text{ cm}^{-1}$ ) and the peak was possibly overlapped with the medium peak of C-H stretching for the alkene group ( $3100\text{--}3000\text{ cm}^{-1}$ ). Strong hydrogen bonding between O-H groups may explain the extension of stretching vibration to  $3000\text{ cm}^{-1}$ . A doublet peak is observed at  $2926.01$  and  $2877.79\text{ cm}^{-1}$ . That doublet peak could be attributed to the asymmetric and symmetric C-H stretching of saccharides in honey. The presence of the aldehyde group is further proven by the detection of C=O stretching at  $1735.93\text{ cm}^{-1}$ . C-H bending is also noticed at  $1450\text{ cm}^{-1}$  for methyl,  $1348.24\text{ cm}^{-1}$  for alcohol or phenol, and  $1244.09\text{ cm}^{-1}$  for C-N stretching of the amine group. A strong S=O stretching can be seen at  $1029.99\text{ cm}^{-1}$  which is most probably contributed by sulfur containing protein in honey. Honey was reported to have approximately 0.5% protein [11]. Another small peak which is assigned to be C-O stretching is observed at  $1103.28\text{ cm}^{-1}$  located at the shoulder of the strong peak. This is also a characteristic vibration of C-O in carbohydrates either for aliphatic ether or alcohol group.

The wavenumber between  $1500$  and  $750\text{ cm}^{-1}$  corresponds to the most sensitive absorption region of major components such as honey sugar (about 60–75%) and organic acids [12]. The contribution of sucrose, glucose and fructose is shown by characteristic bands in the region between  $1500$  and  $900\text{ cm}^{-1}$ . Another important spectral wavenumber located at  $900\text{--}750\text{ cm}^{-1}$  is characteristic region for the saccharide configuration [13]. There is a band approximately at  $920\text{ cm}^{-1}$  assigned to the bending vibration of C=C group. The last region, which is very distinctive in the evaluation and description of honey, peaks in the wavenumber of  $890$  to  $810\text{ cm}^{-1}$ , which is the characteristic vibration for anomeric region of carbohydrates or C-H deformation. Figure 3d is the spectrum of curcumin-loaded nanoemulsion consisted of coconut oil and honey as a base in the formulation, in addition to the presence of Tween 80, PEG and glycerol.

### 3.3. Antioxidant Activity

The scavenging capacity of nano-encapsulated curcumin and free curcumin was in a dose-dependent manner ranging from 1 to 45 ppm, as presented in Figure 4. Encapsulation was found to

decrease its scavenging activity, especially at low concentration (<15 ppm). However, the scavenging activity of both samples was observed to be comparable within the concentration of 15–35 ppm.

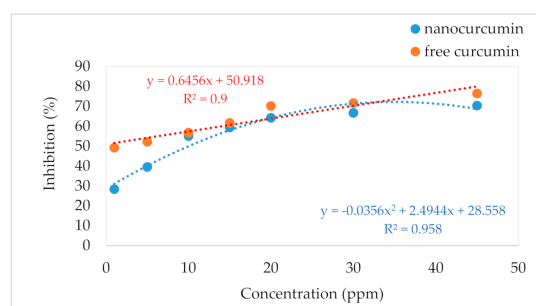


**Figure 4.** Inhibition of 2,2 diphenyl-1-picrylhydrazyl (DPPH) free radicals by curcumin in nanoemulsion (blue line) and free curcumin (red line) at different concentrations.

### 3.4. Skin Permeation and Deposition Study

In vitro skin permeation was carried out using rat skin in a Franz diffusion cell. Curcumin permeated through rat skin and accumulated in the receptor. Solution in the receptor was sampled and analyzed in order to determine the efficiency of nano-encapsulated curcumin in skin permeation. From the results of samples collected from the receptor, nano-sized curcumin permeated into skin faster than free curcumin. The flux rate of nano-sized curcumin was higher than free curcumin. The deposited curcumin in skin was then viewed under a fluorescent microscope after dyed with Nile red (9-diethylamino-5H-benzo[ $\alpha$ ]phenoxazine-5-one), as shown in Figure 5. Nile red is a lipophilic stain and it can be intensely fluorescent in the lipid rich environment of rat skin. The figure clearly shows the penetration of curcumin from the stratum corneum into the epidermis layer after 3 h. The curcumin is then permeated and deposited in the dermis layer after 5 h.

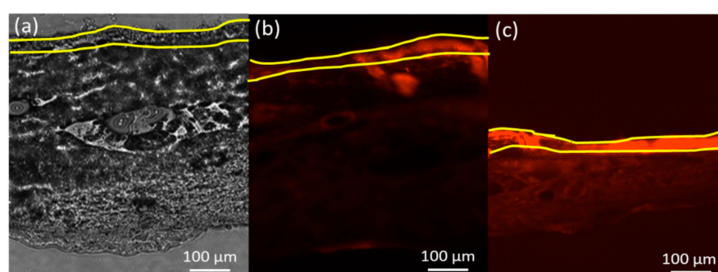


**Figure 5.** Localization of Nile red dyed curcumin-loaded nanoemulsion under fluorescent microscopy on rat skin (a) without treatment, (b) after 3 h of treatment and (c) after 5 h of treatment.

### 3.5. Release Kinetics

The release kinetics of encapsulated curcumin was evaluated based on the cumulative amount of curcumin released from nanoemulsion and consequently permeated through rat skin into the receiver of a Franz diffusion cell. Samples were withdrawn at time interval for 24 h. The data were analysed and plotted using five kinetic models such as zero, first, second, Higuchi, and Korsmeyer–Peppas equations. Table 1 lists the kinetic constant and goodness of the fit in terms of the correlation coefficient,  $r^2$ , for the kinetic models. The results found that both Higuchi and Korsmeyer–Peppas models could fit well into the data satisfactorily. The model achieves the highest correlation coefficient (>0.9) for both free curcumin and encapsulated curcumin.

**Table 1.** Release kinetics of free curcumin and encapsulated curcumin in nanoemulsion during transdermal delivery on rat skin.

Order	Kinetic Model	Linearized Kinetic Model	Constant (k)		Correlation Coefficient (r <sup>2</sup> )	
			Free Curcumin	Curcumin Nanoemulsion	Free Curcumin	Curcumin Nanoemulsion
<b>Zero</b>	$C_t - C_o = k.t$	$C_t = C_o - k.t$	0.5701 mg/h	0.806 mg/h	0.7867	0.8112
<b>First</b>	$\frac{C_t}{C_o} = e^{-k.t}$	$\ln C_t = \ln C_o - k.t$	0.0674 mg/h	0.0706 mg/h	0.5291	0.4908
<b>Second</b>	$C_t = \frac{C_o}{1+k.t.C_o}$	$\frac{1}{C_t} = k.t + \frac{1}{C_o}$	0.0062 mg <sup>-1</sup> .h <sup>-1</sup>	0.0048 mg <sup>-1</sup> .h <sup>-1</sup>	0.3244	0.2893
<b>Higuchi</b>	$Q = k.t^{1/2}$	$Q = k.t^{1/2}$	0.3101 mg.h <sup>-1/2</sup>	0.2225 mg.h <sup>-1/2</sup>	0.9533	0.9512
<b>Korsmeyer–Peppas</b>	$\frac{M_t}{M_\infty} = k.t^n$	$\log\left(\frac{M_t}{M_\infty}\right) = n \log t + \log k$	n = 0.2965, k = 0.6531 h <sup>-n</sup>	n = 0.3057, k = 0.8816 h <sup>-n</sup>	0.9867	0.9695

$C_o$ : initial concentration;  $C_t$ : concentration at time  $t$ ;  $t$ : permeation time;  $k$ : kinetic constant;  $Q$ : analyte flux (mg/cm<sup>2</sup>/h);  $M_t$  is the amount of drug released in time  $t$ ;  $M_\infty$  is the amount of drug released after time  $\infty$ ;  $n$  is the diffusional or release exponent.

### 3.6. Performance on Wound Closure by Scratch Assay

Figure 6 shows the percentage of wound closure promoted by fibroblasts after being treated with nano-encapsulated curcumin at different concentrations for 6, 12 and 24 h. The images of cell proliferation and migration are taken and presented in Figure 7. A low concentration of nano-encapsulated curcumin (0.1563  $\mu\text{g}/\text{mL}$ ) showed to have comparable performance with ascorbic acid (5  $\mu\text{g}/\text{mL}$ ) in wound closure after 24 h. The nano-encapsulated curcumin was found to improve wound closure slightly more than the negative control. However, a higher concentration of nano-encapsulated curcumin did not promote cell migration and the images showed to have cell blebbing and bubbling at the concentration of 1.25  $\mu\text{g}/\text{mL}$ . The cell image of Figure 7f shows died fibroblasts after treatment with a high concentration (2.5  $\mu\text{g}/\text{mL}$ ) of curcumin-loaded nanoemulsion.

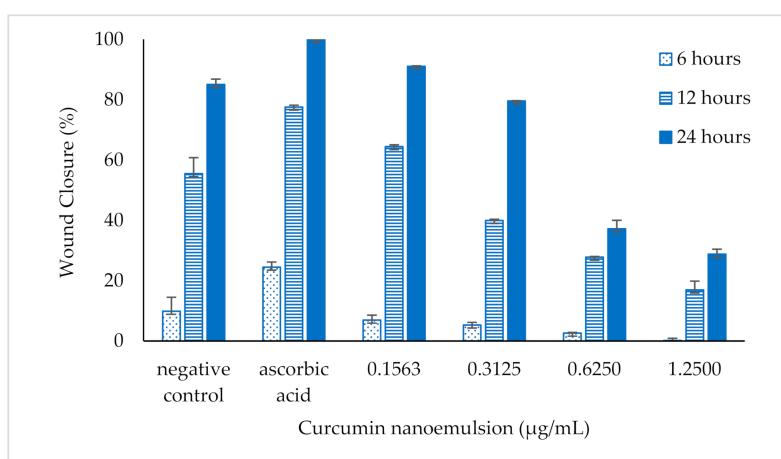


**Figure 6.** Wound closure based on the migration of fibroblasts after 6 (dot bar), 12 (line bar) and 24 (solid bar) hours of treatment. One way analysis of variance was performed to indicate that the results of samples (0.1563–1.25  $\mu\text{g}/\text{mL}$ ) were significantly different ( $p < 0.05$ ) against the negative (untreated) and positive (ascorbic acid) controls at 6, 12 and 24 h of treatment.

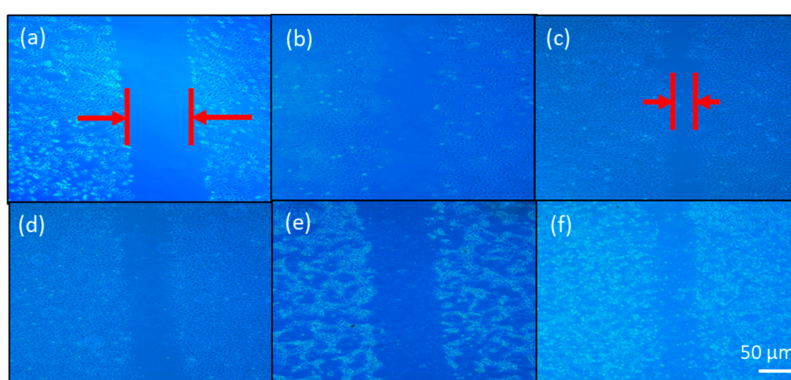


**Figure 7.** Images of fibroblast migration without (a) and with the 24 h treatment of curcumin nanoemulsion at the concentration of (b) 0.1563, (c) 0.3125, (d) 0.6250, (e) 1.2500 and (f) 2.5000  $\mu\text{g}/\text{mL}$ .

### 3.7. Cytotoxic Study

In the present study, HSF cells were treated with samples at the concentration range 0.1563–2.50  $\mu\text{g}/\text{mL}$ . The viability of cells was decreased in a concentration-dependent manner as presented in Figure 8. The decrease could be attributed to the presence of 3% glycerol in nanoemulsion because Wiebe and Dinsdale [14] did report that the inhibition of cell proliferation was significantly decreased at the concentration of glycerol from 2 to 4%. The results show that both curcumin and curcumin nanoemulsion were considered to be non-toxic (>70% cell viability) at the concentration lower than 1.25  $\mu\text{g}/\text{mL}$  after 24 h of treatment [15]. However, the cell viability was dropped to less than 50% at a

high concentration, 2.5  $\mu\text{g}/\text{mL}$ . The  $\text{EC}_{50}$  of free curcumin and nano-encapsulated curcumin were 2.5625 and 2.3552  $\mu\text{g}/\text{mL}$ , respectively.

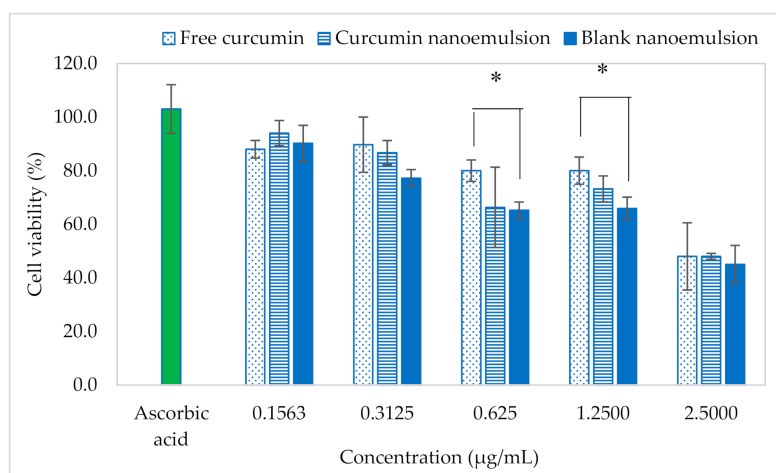


**Figure 8.** Cell viability of ascorbic acid (green bar), free curcumin (dot bar), curcumin-loaded nanoemulsion (line bar) and blank nanoemulsion (solid bar) on human skin fibroblasts after 24 h of treatment. The cell viability of samples between free curcumin or curcumin nanoemulsion and blank nanoemulsion was compared using one-way analysis of variance. \* indicates that the mean of the data is significantly different ( $p < 0.05$ ).

#### 4. Discussion

The pseudoternary phase diagram clearly explains that the increase of VCO content would increase the particle size of nanoemulsion and also increase the required amount of Tween 80 accordingly. The results found that 1% VCO required at least 3% Tween 80 for the formation of oil-in-water nanoemulsion. The ratio of oil to surfactant indicates the coverage of oil droplet by surfactant, which has a direct influence on the emulsion stability. The formulation in the large existence area of nanoemulsion domain was selected to prepare a clear and translucent curcumin-loaded nanoemulsion.

The key ingredient VCO is rich in medium-chain saturated fatty acids and is a good oil for human health, and honey mostly consists of monosaccharides, which could be a natural stabilizer for nanoemulsion. Hence, curcumin, which is also an oil-soluble pigment could be stabilized by the addition of honey and glycerol. Besides being stabilizers, honey and glycerol could also assist in nanoemulsion formation. Honey and glycerol are polyols with higher density than water. The addition of polyols could minimize the difference of phase density between oil and aqueous phases, and therefore more stable nanoemulsion could be formed [16]. Although curcumin is well known for its therapeutic property, it has poor stability in stomach at acidic condition and thus low performance of bioavailability in medical treatment. Encapsulating nano-sized curcumin could enhance curcumin solubility and bioavailability.

Curcumin is a natural polyphenol and chemically known as diferuloylmethane ( $\text{C}_{21}\text{H}_{20}\text{O}_6$ ), with the molecular mass of 368.37 g/mol. There are two aryl rings containing orthomethoxy phenolic OH-groups, which are symmetrically linked to a  $\beta$ -diketone moiety. Curcumin can co-exist with several tautomeric forms, of which two predominant forms are 1,3-diketo form and 1,3-dienol form. No degradation can be spotted in the FTIR spectrum as the signature peaks of pure curcumin still can be found in the sample of curcumin-loaded nanoemulsion.

Encapsulation might hinder the movement of the electron donated by antioxidative curcumin to scavenge free radicals. The hindrance could be explained by the mass transfer limitation, which can be seen from the parabolic behavior of inhibition against nano-encapsulated curcumin concentration. A small difference of reduction in antioxidant activity was also reported by Sari et al. [4], who demonstrated that the total antioxidant activity of curcumin nanoemulsion was reduced from 3.53

to 3.33  $\mu\text{M}$  Trolox/mg of curcumin after encapsulation. On the other hand, the scavenging capacity of free curcumin was found to be linearly increased with the increase in curcumin concentration.

The kinetics of curcumin was a diffusion-controlled release of permeation [17]. The Korsmeyer-Peppas model was used to further explain the mechanism of curcumin release. The release was found to follow Fickian diffusion as the release exponent was 0.3 ( $<0.5$ ) [18]. This means that curcumin diffused at a comparatively slower rate, as the diffusion time was longer based on the square root kinetic of the Korsmeyer-Peppas model. The release kinetic of curcumin was unlikely affected by encapsulation in nanoemulsion as the Korsmeyer constant was not decreased even after nano-encapsulation. The release profile of curcumin was also found to be close to the zero-order kinetic model, indicating that curcumin was nearly independent of its concentration, especially after nano-encapsulation with higher correlation coefficient and kinetic constant.

Scratch assay is a rapid and inexpensive in vitro screening method to verify the effectiveness of samples for wound healing property. This assay examines the second phase of wound healing process characterized by the proliferation and migration of fibroblasts [19,20]. The findings are in agreement with those of de Campos et al. [21], who observed that high doses of curcumin-loaded nanoemulsion promoted cell death. This indicates that curcumin-loaded nanoemulsion has a cytotoxic potential at the concentration higher than 1.2500  $\mu\text{g/mL}$ .

Skin acts as the first barrier to protect the body against external stimuli from the environment. Therefore, HSF is usually used to determine toxicity of natural products and their active compounds which influence the migration of fibroblasts to improve the cutaneous wound healing progression. The cytotoxicity of curcumin against fibroblasts was not significantly affected even after nano-encapsulation.

## 5. Conclusions

This study demonstrated the preparation and characterization of curcumin-loaded nanoemulsion using coconut oil and honey as oil and aqueous phases, respectively. The encapsulation of nano-sized curcumin appeared to improve skin permeation and kinetic release. The curcumin nanoemulsion was considered to be cytotoxic to fibroblasts at the concentration higher than 1.25  $\mu\text{g/mL}$ . A low concentration (0.1563  $\mu\text{g/mL}$ ) of curcumin nanoemulsion was found to promote wound closure in which the performance was comparable with the result of ascorbic acid (5  $\mu\text{g/mL}$ ). The antioxidant capacity expressed in free radical scavenging activity was slightly decreased after nanoemulsification, most probably due to the mass transfer limitation.

**Author Contributions:** Conceptualization, L.S.C.; methodology, R.H.; software, N.H.M.S.; validation, L.S.C. and R.H.; formal analysis, N.H.M.S. and L.Y.; investigation, N.H.M.S.; data curation, L.Y.; writing—original draft preparation, N.H.M.S.; writing—review and editing, L.S.C.; visualization, L.Y.; supervision, L.S.C. and R.H.; project administration, L.S.C.; funding acquisition, L.S.C. All authors have read and agreed to the published version of the manuscript.

**Funding:** This research was funded by the Ministry of Higher Education, Malaysia, under the grant number of HICoE 4]263.

**Acknowledgments:** Technical support from the technicians of IBD laboratory.

**Conflicts of Interest:** The authors declare no conflict of interest.

## References

1. Hashish, E.A.; Elgaml, S.A. Hepatoprotective and nephroprotective effect of curcumin against copper toxicity in rats. *Indian. J. Clin. Biochem.* **2016**, *31*, 270–277. [[CrossRef](#)] [[PubMed](#)]
2. Nagahama, K.; Utsumi, T.; Kumano, T.; Maekawa, S.; Oyama, N.; Kawakami, J. Discovery of a new function of curcumin which enhances its anticancer therapeutic potency. *Sci. Rep.* **2016**, *6*, 30962. [[CrossRef](#)] [[PubMed](#)]
3. Azami, S.J.; Teimouri, A.; Keshavarz, H.; Amani, A.; Esmaeili, F.; Hasanpour, H.; Elikae, S.; Salehiniya, H.; Shojaee, S. Curcumin nanoemulsion as a novel chemical for the treatment of acute and chronic toxoplasmosis in mice. *Int. J. Nanomed.* **2018**, *13*, 7363–7374. [[CrossRef](#)] [[PubMed](#)]

4. Sari, T.P.; Mann, B.; Kumar, R.; Singh, R.R.B.; Sharma, R.; Bhardwaj, M.; Athira, S. Preparation and characterization of nanoemulsion encapsulating curcumin. *Food Hydrocoll.* **2015**, *43*, 540–546. [[CrossRef](#)]
5. Rachmawati, H.; Budiputra, D.K.; Mauludin, R. Curcumin nanoemulsion for transdermal application: Formulation and evaluation. *Drug Dev. Ind. Pharm.* **2015**, *41*, 560–566. [[CrossRef](#)] [[PubMed](#)]
6. Ahmad, N.; Ahmad, R.; Al-Qudaihi, A.; Alaseel, S.E.; Fita, I.Z.; Khalid, M.S.; Pottou, F.H. Preparation of a novel curcumin nanoemulsion by ultrasonication and its comparative effects in wound healing and the treatment of inflammation. *RSC. Adv.* **2019**, *9*, 20192–20206. [[CrossRef](#)]
7. Guerrero, S.; Inostroza-Riquelme, M.; Contreras-Orellana, P.; Diaz-Garcia, V.; Lara, P.; Vivanco-Palma, A.; Cárdenas, A.; Miranda, V.; Robert, P.; Leyton, L.; et al. Curcumin-loaded nanoemulsion: A new safe and effective formulation to prevent tumor recurrence and metastasis. *Nanoscale* **2018**, *10*, 22612–22622. [[CrossRef](#)]
8. De Matos, R.P.A.; Calmon, M.F.; Amantino, C.F.; Villa, L.L.; Primo, F.L.; Claudio Tedesco, A.; Rahal, P. Effect of curcumin-nanoemulsion associated with photodynamic therapy in cervical carcinoma cell lines. *BioMed. Res. Int* **2018**, *2018*, 4057959. [[CrossRef](#)] [[PubMed](#)]
9. Mohan, P.K.; Sreelakshmi, G.; Muraleedharan, C.V.; Joseph, R. Water soluble complexes of curcumin with cyclodextrins: Characterization by FT-Raman spectroscopy. *Vib. Spectrosc.* **2012**, *62*, 77–84. [[CrossRef](#)]
10. Guillén, M.D.; Cabo, N. Characterization of edible oils and lard by fourier transform infrared spectroscopy. Relationships between composition and frequency of concrete bands in the fingerprint region. *J. Am. Oil. Chem. Soc.* **1997**, *74*, 1281–1286. [[CrossRef](#)]
11. Bogdanov, S.; Jurendic, T.; Sieber, R.; Gallmann, P. Honey for nutrition and health: A review. *J. Am. Coll. Nutr.* **2008**, *27*, 677–689. [[CrossRef](#)] [[PubMed](#)]
12. Machado De-Melo, A.A.; Almeida-Muradian, L.B.D.; Sancho, M.T.; Pascual-Maté, A. Composition and properties of *Apis mellifera* honey: A review. *J. Apicul. Res.* **2018**, *57*, 5–37. [[CrossRef](#)]
13. Kędzierska-Matysek, M.; Matwijczuk, A.; Florek, M.; Barłowska, J.; Wolanciuk, A.; Matwijczuk, A.; Chruściel, E.; Walkowiak, R.; Karcz, D.; Gładyszewska, B. Application of FTIR spectroscopy for analysis of the quality of honey. *BIO Web Conf.* **2018**, *10*, 02008.
14. Wiebe, J.P.; Dinsdale, C.J. Inhibition of cell proliferation by glycerol. *Life Sci.* **1991**, *48*, 1511–1517. [[CrossRef](#)]
15. ISO10993-5. *Biological Evaluation of Medical Devices—Part. 5: Tests for In Vitro Cytotoxicity*, 3rd ed.; International Standard: Geneva, Switzerland, 2009; p. 34.
16. Zhang, W.; Zhu, D.; Qin, Y.; Ou, W.; Bao, Y.; Song, L.; Zhang, Q. Effects of compositions on the stability of polyols-in-oil-in-water (P/O/W) multiple emulsions. *J. Disper. Sci. Technol.* **2017**, *39*, 1344–1351. [[CrossRef](#)]
17. Aniesrani Delfiyaa, D.S.; Thangavel, K. Evaluation of in vitro release pattern of curcumin loaded egg albumin nanoparticles prepared using acetone as desolvation agent. *Curr. Tr. Biotechnol. Pharm.* **2016**, *10*, 125–135.
18. Wojcik-Pastuszka, D.; Krzak, J.; Macikowski, B.; Berkowski, R.; Osiński, B.; Musiał, W. Evaluation of the release kinetics of a pharmacologically active substance from model intra-articular implants replacing the cruciate ligaments of the knee. *Materials* **2019**, *12*, 1202. [[CrossRef](#)]
19. Schäfer, M.; Werner, S. Transcriptional control of wound repair. *Annu. Rev. Cell Dev. Biol.* **2007**, *23*, 69–92. [[CrossRef](#)]
20. Liu, M.L.; Zang, T.; Zou, Y.; Chang, J.C.; Gibson, J.R.; Huber, K.M.; Zhang, C.L. Small molecules enable neurogenin 2 to efficiently convert human fibroblasts into cholinergic neurons. *Nat. Comm.* **2013**, *4*, 1–10. [[CrossRef](#)] [[PubMed](#)]
21. De Campos, P.S.; Matte, B.F.; Diel, L.F.; Jesus, L.H.; Bernardi, L.; Alves, A.M.; Rados, P.V.; Lamers, M.L. Low doses of curcuma longa modulates cell migration and cell–cell adhesion. *Phytother. Res.* **2017**, *31*, 1433–1440. [[CrossRef](#)] [[PubMed](#)]

